

# Teflon-coated microfiber resonator with weak temperature dependence

Ye Chen,<sup>1</sup> Fei Xu,<sup>1,\*</sup> and Yan-qing Lu<sup>1,2</sup>

<sup>1</sup>College of Engineering and Applied Sciences and National Laboratory of Solid State Microstructures, Nanjing University, Nanjing 210093, China

<sup>2</sup>yqlu@nju.edu.cn  
feixu@nju.edu.cn

**Abstract:** A temperature insensitive three-turn microfiber coil resonator (MCR) is demonstrated by embedding it in Teflon with opposite thermo-optic coefficient. The temperature dependence of a MCR strongly depends on the microfiber size which controls the ratio of thermal effect contributions from silica and polymer. Fabricated from a  $\sim 3\mu\text{m}$ -diameter microfiber, the temperature dependence of our MCR is compensated to less than  $6\text{pm}/^\circ\text{C}$ . Further suppression of the temperature dependence can be realized with ideal microfiber radius.

©2011 Optical Society of America

**OCIS codes:** (060.2370) Fiber optics sensors; (120.6780) Temperature.

---

## References and links

1. G. Brambilla, "Optical fibre nanotaper sensors," *Opt. Fiber Technol.* **16**(6), 331–342 (2010).
2. G. Brambilla, "Optical fibre nanowires and microwires: a review," *J. Opt.* **12**(4), 043001 (2010).
3. Y. M. Jung, G. S. Murugan, G. Brambilla, and D. J. Richardson, "Embedded optical microfiber coil resonator with enhanced High Q," *IEEE Photon. Technol. Lett.* **22**, 1638–1640 (2010).
4. X. S. Jiang, L. M. Tong, G. Vienne, X. Guo, A. Tsao, Q. Yang, and D. R. Yang, "Demonstration of optical microfiber knot resonators," *Appl. Phys. Lett.* **88**(22), 223501 (2006).
5. G. Vienne, A. Coillet, P. Grelu, M. El Amraoui, J.-C. Jules, F. Smektala, and L. Tong, "Demonstration of a reef knot microfiber resonator," *Opt. Express* **17**(8), 6224–6229 (2009).
6. F. Xu and G. Brambilla, "Embedding optical microfiber coil resonators in Teflon," *Opt. Lett.* **32**(15), 2164–2166 (2007).
7. N. G. Broderick, "Optical snakes and ladders: dispersion and nonlinearity in microcoil resonators," *Opt. Express* **16**(20), 16247–16254 (2008).
8. M. Sumetsky, "Optical fiber microcoil resonator," *Opt. Express* **12**(10), 2303–2316 (2004).
9. F. Xu and G. Brambilla, "Manufacture of 3-D microfiber coil resonators," *IEEE Photon. Technol. Lett.* **19**(19), 1481–1483 (2007).
10. L. M. Tong, R. R. Gattass, J. B. Ashcom, S. L. He, J. Y. Lou, M. Y. Shen, I. Maxwell, and E. Mazur, "Subwavelength-diameter silica wires for low-loss optical wave guiding," *Nature* **426**(6968), 816–819 (2003).
11. F. Xu and G. Brambilla, "Demonstration of a refractometric sensor based on optical microfiber coil resonator," *Appl. Phys. Lett.* **92**(10), 101126 (2008).
12. R. Lorenzi, Y. M. Jung, and G. Brambilla, "In-line absorption sensor based on coiled optical microfiber," *Appl. Phys. Lett.* **98**(17), 173504 (2011).
13. T. Lee, N. G. R. Broderick, and G. Brambilla, "Transmission properties of microcoils based on twisted birefringent fibre," *Opt. Commun.* **284**(7), 1837–1841 (2011).
14. G. Brambilla, F. Xu, P. Horak, Y. Jung, F. Koizumi, N. P. Sessions, E. Koukharenko, X. Feng, G. S. Murugan, J. S. Wilkinson, and D. J. Richardson, "Optical fiber nanowires and microwires: fabrication and applications," *Adv. Opt. Photon.* **1**(1), 107–161 (2009).
15. X. Zeng, Y. Wu, C. Hou, J. Bai, and G. Yang, "A temperature sensor based on optical microfiber knot resonator," *Opt. Commun.* **282**(18), 3817–3819 (2009).
16. "Teflon® AF properties," [http://www2.dupont.com/Teflon\\_Industrial/en\\_US/products/product\\_by\\_name/teflon\\_af/properties.html](http://www2.dupont.com/Teflon_Industrial/en_US/products/product_by_name/teflon_af/properties.html).
17. "Teflon," <http://www.lenntech.com/teflon.htm>.
18. S. T. Chu, W. Pan, S. Suzuki, B. E. Little, S. Sato, and Y. Kokubun, "Temperature insensitive vertically coupled microring resonator add/drop filters by means of a polymer overlay," *IEEE Photon. Technol. Lett.* **11**(9), 1138–1140 (1999).
19. G. Brambilla, V. Finazzi, and D. Richardson, "Ultra-low-loss optical fiber nanotapers," *Opt. Express* **12**(10), 2258–2263 (2004).
20. J. Teng, P. Dumon, W. Bogaerts, H. Zhang, X. Jian, X. Han, M. Zhao, G. Morthier, and R. Baets, "Athermal silicon-on-insulator ring resonators by overlaying a polymer cladding on narrowed waveguides," *Opt. Express* **17**(17), 14627–14633 (2009).

21. F. Xu, P. Horak, and G. Brambilla, "Optical microfiber coil resonator refractometric sensor," *Opt. Express* **15**(12), 7888–7893 (2007).
22. F. Xu, P. Horak, and G. Brambilla, "Optical microfiber coil resonator refractometric sensor: erratum," *Opt. Express* **15**(15), 9385 (2007).
23. F. Xu, V. Pruneri, V. Finazzi, and G. Brambilla, "An embedded optical nanowire loop resonator refractometric sensor," *Opt. Express* **16**(2), 1062–1067 (2008).

## 1. Introduction

Optical micro-resonators have generated tremendous research progress in telecommunication and sensing with key merits of compact size, wavelength agility and tunability. Various micro-resonators have been investigated and demonstrated, including photonic crystal cavities, ring resonators, microspheres and optical microfiber coil resonators (MCRs) [1–10]. As a basic functional element of the microfiber photonic circuit, MCRs in forms of self-coupling loop, knot and 3D coil structures [1–10] have increasingly attracted interest due to their intrinsic advantages of small scattering/absorption loss, structural simplicity and direct coupling to input/output fibers, following the quick development of fabrication technology on subwavelength-diameter microfibers. In particular the 3D MCR is a difficulty for standard planar light circuit (PLC) technology due to the stereoscopic geometry. However, it could be easily obtained by just wrapping a microfiber on a low index dielectric rod. Taking the benefit of the unique structure, the 3D MCR can be employed as a highly sensitive microfluidic sensor [11,12], a current sensor, an optical gyroscopes, a berry phase magnifier, a temperature sensor, a slow light generator or an optical signal processor [13,14]. For the deployment of the MCR, investigation of practical implementation issues such as stability, degradation and cleanness is needed to test the robustness of the device. The embedding of a MCR in a low refractive index medium seems to be necessary and the best method to solve reliability issues, providing both protection from fast aging and geometrical stability [3,6]. However, another key issue on temperature stability has not been investigated and solved. For a silica-MCR without polymer coating, the temperature sensitivity is about 10-20pm/°C similar to planar silica ring resonators without polymer cladding. Because the MCR must be embedded in low index polymer in real applications, strong temperature dependent wavelength shifts exist resulting from the thermal expansion and thermo-optic effect of both the fiber and polymer. Ref. [15] reported a knot MCR embedded in low index polymer EFIRON UVF which has a sensitivity of ~300pm/°C. It is useful for temperature sensing but harmful to most sensing and telecom applications.

In this paper, we investigate theoretically and experimentally the thermal characteristics of a 3D MCR embedded in Teflon. Our calculation shows that the temperature dependence severely relates to the microfiber diameter and it is possible to suppress the temperature dependence at a certain diameter. By embedding a three-turn MCR with ~3µm-diameter microfiber in Teflon, we demonstrate the temperature-dependent wavelength shift as low as ~6pm/°C in the room temperature range. Weaker temperature-dependence can be achieved by controlling the microfiber diameter precisely.

## 2. Theory

In a MCR embedded in low index polymer, the main resonance condition can be expressed as

$$2\pi n_{\text{eff}} / \lambda_r L = \text{Constant} \quad (1)$$

where  $n_{\text{eff}}$ ,  $\lambda_r$  and  $L$  are the effective refractive index, resonance wavelength and coil length, respectively.

The resonance wavelength temperature dependence of a MCR embedded in a low index polymer is

$$S = d\lambda_r/dT = S_{TOE,MF} + S_{TOE,LP} + S_{TEE,MF} + S_{TEE,LP}$$

$$\begin{cases} S_{TOE,MF} = (\lambda_r/n_{eff})\sigma_{MF} (\partial n_{eff}/\partial n_{MF}) \\ S_{TOE,LP} = (\lambda_r/n_{eff})\sigma_{LP} (\partial n_{eff}/\partial n_{LP}) \\ S_{TEE,MF} = (\lambda_r/n_{eff})\alpha_{MF} (n_{eff} + r \partial n_{eff}/\partial r) \\ S_{TEE,LP} = \gamma\alpha_{LP}\lambda_r \end{cases} \quad (2)$$

where  $S_{TOE,MF}$  ( $S_{TOE,LP}$ ) and  $S_{TEE,MF}$  ( $S_{TEE,LP}$ ) are contributions from thermo-optic and thermal expansion effects of the microfiber (low index polymer, LP).  $\alpha_{MF}$  ( $\alpha_{LP}$ ) and  $\sigma_{MF}$  ( $\sigma_{LP}$ ) are the thermal expansion and thermo-optic coefficients of the microfiber (low index polymer).  $r$  is the microfiber radius. For silica microfiber,  $\alpha_{MF} = 5.5 \times 10^{-7} / ^\circ\text{C}$  and  $\sigma_{MF} = 1.1 \times 10^{-5} / ^\circ\text{C}$ . For Teflon®AF,  $\alpha_{LP} \approx 0.8 \times 10^{-4} / ^\circ\text{C}$  and  $\sigma_{LP} \approx -1.3 \times 10^{-4} / ^\circ\text{C}$  [16,17]. Because of the mismatched thermal expansion between silica microfiber and polymer, we induce  $\gamma$  ( $0 < \gamma < 1$ ) in  $S_{TEE,LP}$  which represents the effective contribution on the microfiber coil length from the thermal expansion of polymer.

Figure 1(a) shows the dependence of  $\partial n_{eff}/\partial n_{MF}$  and  $\partial n_{eff}/\partial n_{LP}$  on the microfiber radius using the following parameters: the index of microfiber  $n_c = 1.4443$ , the index of Teflon®AF  $n_t = 1.311$ , the wavelength  $\lambda_r = 1550\text{nm}$ .  $n_{eff}$  is about 1.31 ~1.443 and increases slowly with radius.  $\partial n_{eff}/\partial n_{MF}$  and  $\partial n_{eff}/\partial n_{LP}$  vary quickly with radius when  $r < 1.5\mu\text{m}$ .  $n_{eff}$  is the effective index. All the simulation is performed using Matlab.

According to our calculations, the thermal expansion effect of silica  $S_{TEE,MF}$  contributes little to the total sensitivity and can be ignored. The contribution from thermo-optic effect of silica ( $S_{TOE,MF}$ ) is about 12 - 20 pm/°C which coincides with planar silica ring resonator [18].  $S_{TOE,LP}$  is very important and dominates because the thermo-optic coefficients of Teflon are ten times larger than the thermo-optic effect of silica. It is very difficult to have the accurate value of  $S_{TEE,LP}$ , but as we expect, the multi-turn coils are very tight in the polymer so the polymer lateral expansion inside the coils cannot change the coil length much and the polymer inside the coils mainly expands longitudinally. For simplify, we can assume that  $S_{TEE,LP}$  is very small and ignore it here. At a special radius, the negative thermo-optic effect can compensate other thermal effect with the following athermal condition:

$$-\sigma_{LP} \frac{\partial n_{eff}}{\partial n_{LP}} = \alpha_{MF} (n_{eff} + r \partial n_{eff}/\partial r) + \sigma_{MF} \frac{\partial n_{eff}}{\partial n_{MF}} + \gamma\alpha_{LP}n_{eff} \approx \sigma_{MF} \frac{\partial n_{eff}}{\partial n_{MF}} \quad (3)$$

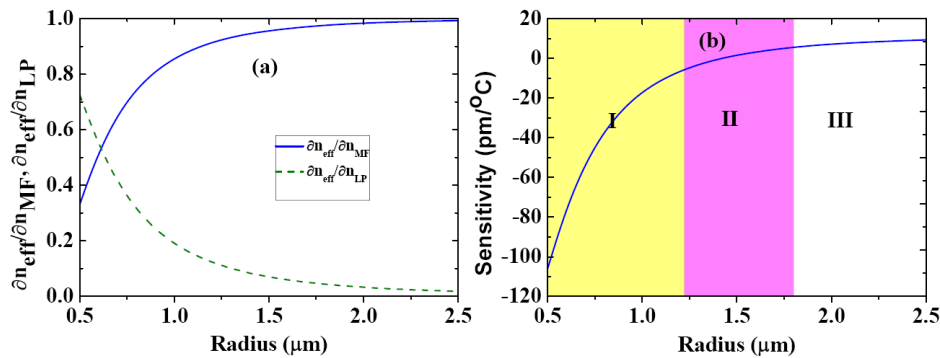


Fig. 1. (a) Variation of  $\partial n_{eff}/\partial n_{MF}$  (solid line) and  $\partial n_{eff}/\partial n_{LP}$  (dashed line) as a function of the microfiber radius. (b) Variation of the estimated sensitivity as a function of the microfiber radius, only considering the contribution from thermo-optic effect. Red area II is the temperature insensitive area where  $|S| < 5\text{pm}/^\circ\text{C}$ .

Figure 1(b) shows the dependence of sensitivity on the microfiber radius only considering the contribution from thermo-optic effect. If we define the temperature insensitive area where  $|S| < 5\text{pm}/^\circ\text{C}$ , the estimated microfiber radius for temperature insensitive MCR is  $\sim 1.45\mu\text{m}$  (red area, II). If the radius is small in the area I, the dominated contribution is from thermo-optic effect of polymer and MCR shows high temperature dependence which coincides with Ref. [15]. If the radius is large in the area III, the dominated contribution is from thermo-optic effect of microfiber and MCR shows medium temperature dependence.

### 3. Fabrication

Our MCR was fabricated using the process and setup presented in [12]. A standard single-mode fiber (Corning SMF-28) was heated and tapered down into a very thin microfiber by using the flame brushing technique [2,14,19]. The microfiber diameter and the length of the uniform waist region were  $\sim 3\mu\text{m}$  and  $\sim 5\text{mm}$ , respectively. The fabricated microfiber was carefully wound onto a Teflon-pre-coated support glass rod to form a three-turn coil with the aid of a microscope and rotation stage. The rod diameter  $D_{\text{rod}}$  was  $\sim 1\text{mm}$ . Then the resonator embedding was carried out using the 601S1-100-6 solution of Teflon®AF (DuPont, United States). The structure was repeatedly covered with the Teflon solution on a Teflon-coated substrate and the solvent was allowed to evaporate. The whole sample was cured in air for several hours. We fabricated the three-turn MCR because it was a typical multi-turn MCR, and more turns possibly made the coil wrapped more tightly on the rod. The fabrication reproducibility depends on the precise control of rod and microfiber diameter and coil pitch, which strongly depends on the performance of fabrication facilities including the micro-heater, liner and rotation stages. With the best facilities (nm resolution stages, highly stable electrical-micro-heater, etc.), the reproducibility will be good.

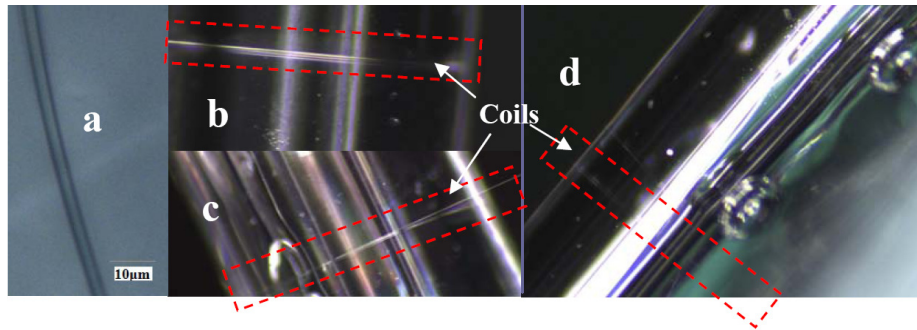


Fig. 2. Microscope pictures of a MCR (a) wrapped on a rod (b), (c) before and (d) after embedded in Teflon. (b) and (c) are taken from different sides. The microfiber and rod radii are  $\sim 1.5$  and  $500\mu\text{m}$ , respectively.

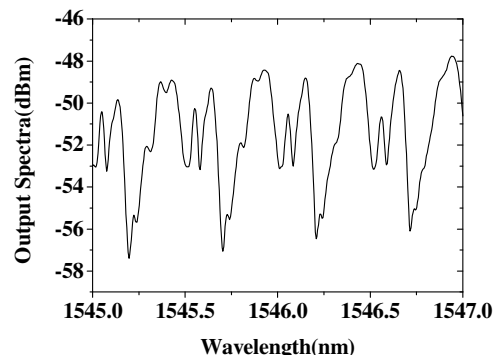


Fig. 3. Transmission spectrum of the embedded MCR onto a 1-mm-diameter support rod in the range from 1545 to 1547 nm.

The microscope pictures of the three-turn MCR before and after embedded in Teflon are shown in Fig. 2. The three-turn coils are very close to each another. Coating with Teflon provides a smooth surface and a homogeneous medium. Although some sporadic bubbles are observed in the polymer, their effect on the MCR is negligible because none of them is in proximity of the microfiber. The transmission spectrum is measured with a broadband source (1525 ~1610nm) and an Ando AQ6317B optical spectrum analyzer (OSA). Figure 3 shows the resonance spectra of the MCR at 23°C. It shows a complicated profile because the coupling among the three turns is possibly irregular and not-exactly uniform and even there is birefringence effect. Here we only consider the main resonance valleys with an extinction ratio of ~9 dB, free spectrum range (FSR) of ~0.51nm, Q factor is ~15,000. Using the simple ring resonator model, the FSR can be written as

$$\text{FSR} = \lambda_r^2 / n_{\text{eff}} L \quad (4)$$

This model predicts FSR ~0.53nm assuming  $L = \pi D_{\text{rod}}$ . The small difference between theoretical prediction and experiments could arise from a real optical path longer than  $\pi D_{\text{rod}}$ , because the microfiber and coil diameters present some irregularity and the coil position is not always perpendicular to the rod which means that the coil diameter is a little bigger than the rod diameter. The transmission spectrum relates on the fiber loss and the coil pitch, It can be improved by reducing the microfiber loss and optimizing the coil pitch, careful optimizations of flame height and stage speed are needed and better facilities are preferred.

We characterize the thermal response of the embedded MCR by heating it up and the temperature ranging from room temperature 23°C to 46°C is measured by a thermocouple (Accuracy 0.1°C, TES-1310, Type K, TES Electrical Electronic Corp.). The spectrum and temperature are recorded when both of them are stable for several minutes.

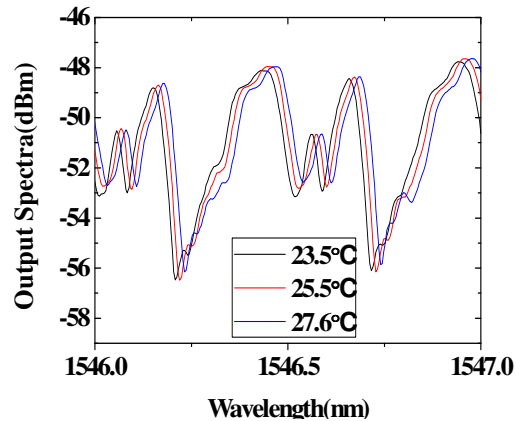


Fig. 4. Transmission spectra of the embedded MCR at three different temperatures.

Figure 4 displays the resonance spectra at three different temperatures 23.5°C, 25.5°C and 27.6°C. As the temperature increases the resonance wavelength shifts to longer wavelength. Figure 5 shows the measured resonance wavelength shifts ( $\Delta\lambda$ ) on temperature ( $T$ ) from 23°C to 46°C. A linear fitting is used across the entire calibration range. The average sensitivity of the device is ~5.8pm/°C and this result shows that the embedded MCR has excellent temperature stability. So far, there are few papers investigating the temperature issues of embedded MCRs, only Ref. [15] reports a temperature sensitivity of ~300pm/°C for a ~1μm-diameter MCR embedded in EFIRON UVF PC-373. Our result is fifty times lower than it, and also comparable with recent results on the athermal silicon-on-insulator ring resonators (~5pm/°C) [20]. Lower sensitivity can be obtained in a MCR with the ideal microfiber size by improving the fabrication technique on longer and more uniform microfiber with precise radius control.

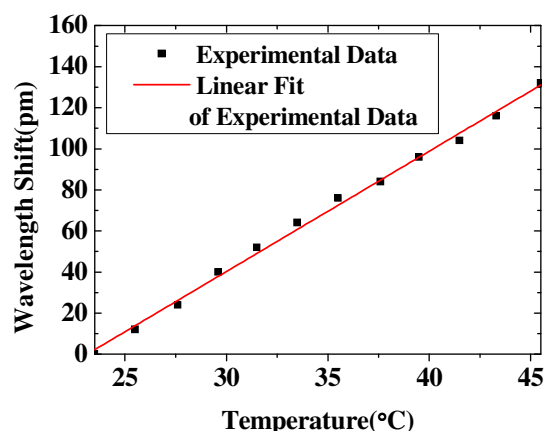


Fig. 5. Variation of the resonance wavelength in the embedded MCR as a function of temperature.

#### 4. Conclusion

In summary, we investigate theoretically and experimentally the thermal characteristics of a MCR embedded in Teflon with negative thermo-optic coefficient. The temperature dependence severely relates to the microfiber radius and it is possible to suppress the temperature dependence at a certain diameter. Our calculation shows that the ideal microfiber radius should be around  $1.45\mu\text{m}$ . By embedding a three-turn MCR with  $\sim 3\mu\text{m}$ -diameter microfiber in Teflon, it shows a low temperature sensitivity of  $< 6\text{pm}/^\circ\text{C}$  in the room temperature range, almost fifty times lower than the  $1\mu\text{m}$ -diameter MCR embedded in EFIRON UVF PC-373. There are several possible reasons on the difference between the design and experimental results: we cannot control the microfiber diameter precisely, our microfiber is not perfectly uniform and the theoretical model ignores the thermal expansion effect. But our experimental results show that the ideal microfiber for temperature insensitivity must be close to  $3\mu\text{m}$ -diameter. If we can control the fiber radius more precisely, we can test a serial of MCRs with different diameters near  $3\mu\text{m}$ , and then find the best diameter. These results are expected to be applied in fabricating temperature-insensitive MCR based filter, refractive index sensor [11,21–23], etc.

#### Acknowledgment

This work is supported by National 973 program under contract No. 2010CB327803, 2011CBA00200 and 2012CB921803, NSFC program No. 11074117 and 60977039, the Fundamental Research Funds for the Central Universities. The authors also acknowledge the support from the Priority Academic Program Development of Jiangsu Higher Education Institutions (PAPD).